

55-39

187836

P-18

N97-19470

Explicit Solution Techniques for Impact with Contact Constraints

Robert E. McCarty
Wright Laboratory
Wright-Patterson Air Force Base, OH



INTRODUCTION

Modern military aircraft transparency systems, windshields and canopies, are complex systems which must meet a large and rapidly growing number of requirements. As illustrated in Fig. 1, many of these transparency system requirements are conflicting, presenting difficult balances which must be achieved. One example of a challenging requirements balance or trade is shaping for stealth versus aircrew vision.

The large number of requirements involved may be grouped in a variety of areas including man-machine interface; structural integration with the airframe; combat hazards; environmental exposures; and supportability. Some individual requirements by themselves pose very difficult, severely nonlinear analysis problems. One such complex problem is that associated with the dynamic structural response resulting from high energy bird impact.

OBJECTIVE:

MISSION
CRITICAL
PERFORMANCE

SUPPORTABILITY
AS A DELIVERABLE
FEATURE

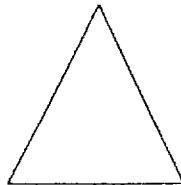


Figure 1 - Balance between performance and supportability requirements for an aircraft transparency system.

¹ Brockman, R. A.; and Held, T. W.: *Explicit Finite Element Method for Transparency Impact Analysis*, WL-TR-91-3006, 1991.

NONLINEAR FINITE ELEMENT ANALYSIS OF AIRCRAFT TRANSPARENCY BIRD IMPACT

Impact phenomena encompass a broad range of structural behavior and response times, which depend upon the stiffness, strength, mass, geometry, velocities, and failure characteristics of the bodies involved. Soft body impacts, such as transparency bird impacts, are unusual: while the response is often highly nonlinear, critical features of the response may occur either at early times or long (milliseconds) after the impact is finished as illustrated in Fig. 2. For over ten years, implicit solution techniques with isoparametric solid finite element technology (Ref. 1) have been used successfully to analyze aircraft transparency bird impact response (Refs. 2-5). An impact solution may be dominated by complicated contact conditions which preclude the use of large time steps, so that the advantages of an implicit solution are lost. Practical transparency analysis remains a time-consuming and laborious process, and in some circumstances the present inventory of analysis tools may not be optimal.

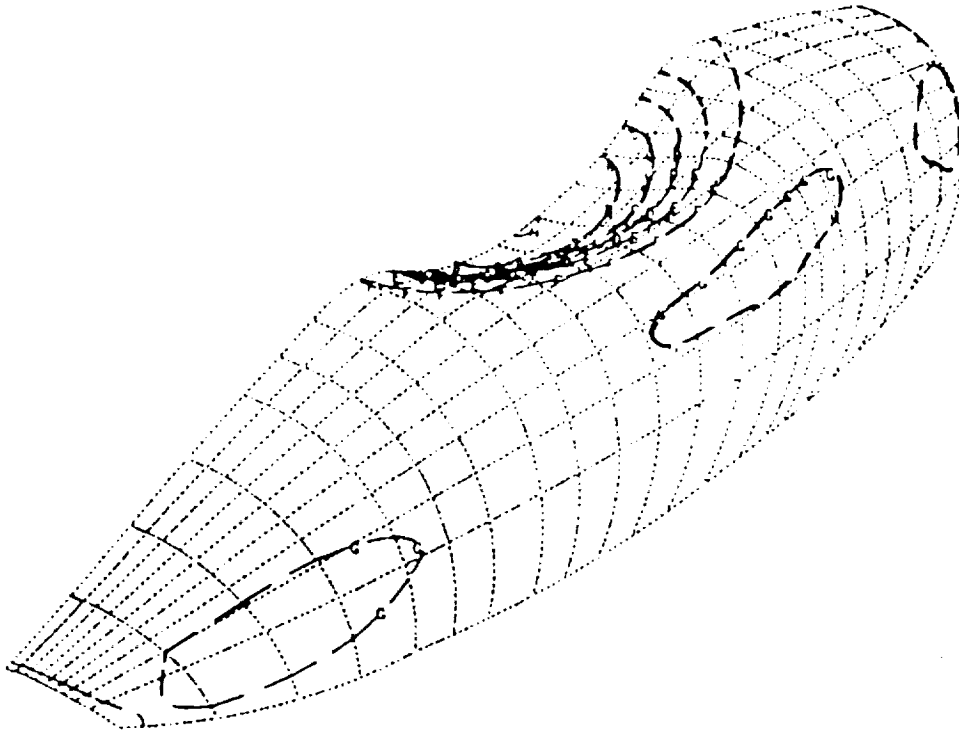


Figure 2 - Dynamic bird impact response of F-16 fighter aircraft prototype canopy design at 20 msec.

EXPLICIT FINITE ELEMENT METHOD FOR AIRCRAFT TRANSPARENCY BIRD IMPACT

This paper outlines the development of new computational techniques for analyzing structural response to high-speed impact. The key improvements in the new technique are listed in Fig. 3. The analytical technique discussed is an explicit finite element method of the type used widely for the numerical solution of shock and wave propagation problems. The explicit family of time integration algorithms is attractive because it is readily adapted to high performance on the current generation of supercomputers, which combine parallel or pipeline processors, moderate amounts of high-speed memory, and relatively slow disk performance. An added benefit is the ability to implement more detailed material and failure models. The particular implementation discussed here is a computer code called X3D. X3D is an explicit, three-dimensional finite element program intended for use in solving impact, wave propagation, and other short-duration problems in structural dynamics.

- *Soft-body impact loads:* the bird appears explicitly in the finite element model, so that ad hoc estimates of the impact loading distribution are unnecessary
- *Material modeling:* the material models include strain rate sensitivity and failure
- *Layered shells:* multilayered constructions, including those with soft interlayers, can be modeled using a single layer of surface elements

Figure 3 - Key improvements offered by explicit finite element methods for nonlinear dynamic aircraft transparency bird impact.

X3D EXPLICIT THREE-DIMENSIONAL FINITE ELEMENT PROGRAM FOR SHORT-DURATION STRUCTURAL DYNAMIC PROBLEMS

X3D contains two types of finite elements: solids and plates. The solid elements are an eight-node hexahedron, based on a mean-stress approximation with anti-hourglass stabilization (Ref. 6); and a four-node tetrahedron. The eight-node solid hexahedron element is illustrated in Fig. 4. The solid hexahedral finite element uses a displacement and velocity approximation based upon trilinear polynomials; that is, the element's displacement and velocity components each vary linearly along each edge of the element. In addition, the stress components are computed from a mean stress approximation using only the mean velocity gradient for the element (Ref. 6). This measure is desirable to maintain good element performance, and also reduces the effort required for element computations. However, the resulting element is a constant stress element, and therefore a generous number may be necessary for accurate modeling. In particular, a single layer of these solids is incapable of developing a bending moment. The material model used for solids consists of a polynomial equation of state coupled with a von Mises plasticity model, a simple power-law correction for strain rate sensitivity, and a failure criterion based upon the ultimate stress.

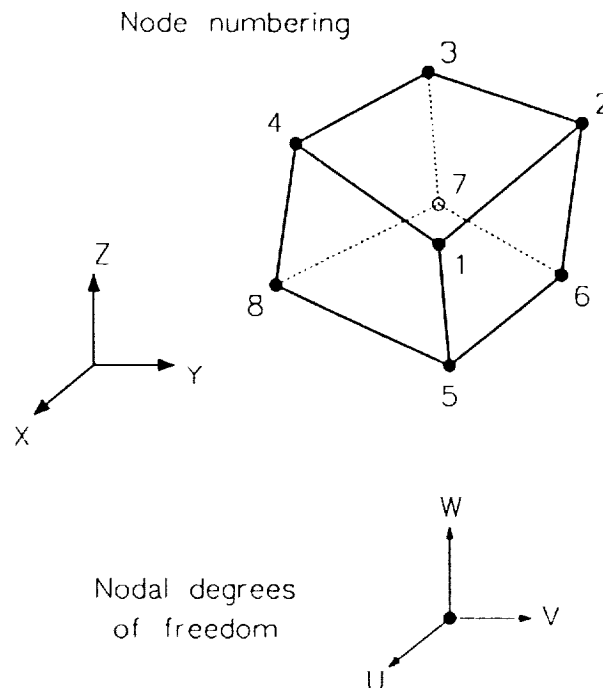


Figure 4 - Eight-node solid hexahedron X3D element.

X3D SOLID HEXAHEDRAL AND TETRAHEDRAL ELEMENTS

Because of the mean stress approximation, certain modes of deformation exist for the hexahedron which are stress-free but do not represent rigid body motions. These hourglassing deformation modes correspond to linearly varying stress patterns which are not detected by the mean stress approximation as shown in Fig. 5. To stabilize these potentially unstable motions, an anti-hourglass viscosity is employed to resist the hourglass motions through internal damping forces (Ref. 7). The tetrahedral solid is a constant-strain, constant-stress element based upon fully linear displacement and velocity field approximations. The element is quite similar to the hexahedron, but does not use an anti-hourglass viscosity. The twelve degrees of freedom for the element capture the six rigid-body motions and the six uniform strain/stress modes, so that no unstable deformation patterns exist for individual elements. The tetrahedron is included in X3D for its utility in soft-body impact modeling. Since the element has no unstable modes, it can be used to follow very large distortions without causing numerical problems. The tetrahedron is used to model the bird in bird impact simulations, using an equation of state typical of water, a very low strength deviatoric model, and an ultimate failure strain of about 5 (500%). The tetrahedron is implemented as a five-node element, the fifth node coinciding with the first. This artifice serves to distinguish the four-node tetrahedron from the four-node quadrilateral plate element during input.

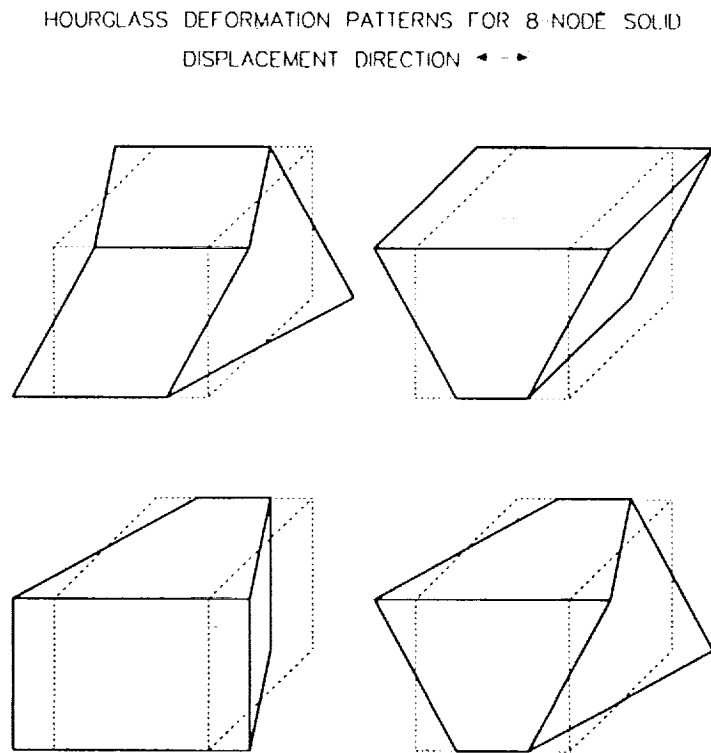


Figure 5 - Hourglass deformation patterns for solid element.

X3D PLATE AND SHELL ELEMENT

The plate and shell element in X3D is a four-node quadrilateral based upon a Mindlin-Reissner type thick-plate theory. A corotational axis system, which rotates with the element but does not deform, is used to simplify the element kinematics. The plate and shell element uses a reduced (one-point) Gaussian quadrature, in conjunction with anti-hourglass stabilization techniques. An approximate model for layered media is implemented for the element, so that plates and shells having layers with large differences in stiffness can be represented effectively using a single element in the thickness direction. For each layer of the X3D plate and shell element, the material is elastic, perfectly plastic, and obeys plane stress assumptions. Transverse shear stresses in the element are uncoupled from the tangential stresses, and follow an elastic constitutive relation. The plate and shell element has six degrees of freedom per node as shown in Fig. 6. The displacement and rotation components each are interpolated separately, using bilinear polynomials. The resulting element is quite similar to that described by Belytschko (Ref. 8).

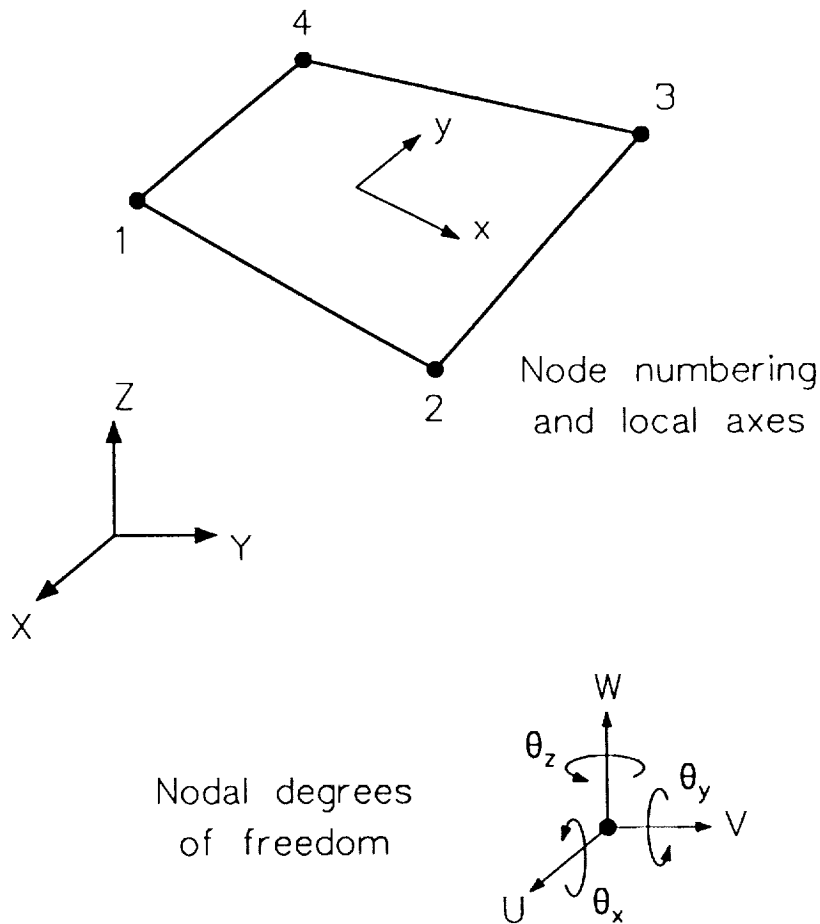


Figure 6 - Four-node quadrilateral plate element.

X3D PLATE AND SHELL ELEMENT

Unlike the solid elements, the plate element must be formulated in a local axis system because of the differing treatment of the plate thickness from that of the planform directions. A corotational coordinate system which rotates with the element is employed, and therefore is constructed anew at each time step of the solution based upon the current element geometry. The plate element shape functions are formulated entirely in local coordinates. The element calculations are performed with respect to the "mean plane" of the element, and corrected as necessary to account for out of plane warping of the reference surface. The plate uses a mean-stress approximation for its inplane directions, similar to the solid hexahedron. At any thickness station, the velocity gradient is evaluated at the centroid of the element, and assumed to be constant throughout the element (except through the thickness). To resist unstable motions resulting from the assumption of a uniform velocity gradient, the plate element uses a stiffness hourglass control scheme (Ref. 6). Other aspects of element design are listed in Fig. 7.

- Simpson's Rule integration through the thickness
- Each layer may be a different material and even use a different material model
- Layered constructions with dramatic stiffness characteristics variation from layer to layer require special treatment
- Formulation of lumped mass coefficients relieves stringent time step restriction without upsetting convergence (Ref. 9)
- No inertia is assigned to the "drilling" rotation in the local coordinate system

Figure 7 - X3D plate and shell element features.

MATERIAL MODELS

The material constitutive relationships used for both the solid and plate finite elements consist of a deviatoric (shear) relation and a bulk (pressure-volume) model. The stress tensor is composed of a hydrostatic, or pressure, stress, and a deviatoric stress tensor which is independent of the pressure. These two contributions to the stress tensor are determined independently in the material model by a deviatoric stress model and a mechanical equation of state. The deviatoric material model used for solids is a rate-dependent, isotropic, hypoelastic theory appropriate for moderate to large deformations. The parameters which define the material's deviatoric behavior are shown in Fig. 8. An experimental feature provides an isotropic Newtonian fluid model for the three-dimensional solid elements for potential use in hydrodynamic impact modeling. The bulk behavior is described in polynomial form as for a solid, while the deviatoric stress is related linearly to the rate of deformation. In the plate element, the elastic-plastic material model is slightly more complicated than for three-dimensional solids because of the zero normal stress constraint. During the plasticity calculation, it is necessary to determine a final state of stress which not only lies on the yield surface, but which satisfies the condition for the normal stress to be zero. The deviatoric model and the bulk model (equation of state) are not entirely independent, and must be solved simultaneously with the normal stress constraint.

- Linear shear modulus
- Quasi-static yield stress
- Rate sensitivity scale factor
- Rate sensitivity exponent
- Hardening modulus
- Ultimate stress

Figure 8 - Parameters for material deviatoric behavior.

LAYERED PLATE AND SHELL MODEL

X3D provides a method of approximation for plates and shells having large stiffness variations from layer to layer, such as those for a laminated aircraft transparency system shown in Fig. 9. Layered structures of this type often require detailed and expensive models, since conventional plate and shell finite elements do not reproduce the correct transverse shear strain distributions through the wall thickness. The X3D method requires only a single layer of elements having six engineering degrees of freedom per node, regardless of the number of layers in the structure. The approximation uses closed-form elasticity solutions to develop transverse shear flexibility corrections, which bring this contribution to the energy into line with that caused by pure bending, twisting, and extension. For large displacement problems, the technique is applied in corotational coordinates. Changes in stiffness caused by plasticity can be accounted for by recomputing the flexibility corrections based upon instantaneous moduli. Applied forces in X3D may consist of body forces and surface pressure. Kinematic boundary conditions may include prescribed nodal displacements, rigid-wall constraints, and contact between specified surfaces within the mesh. Initial conditions may be specified for the translational velocity components for all or part of the finite element model.

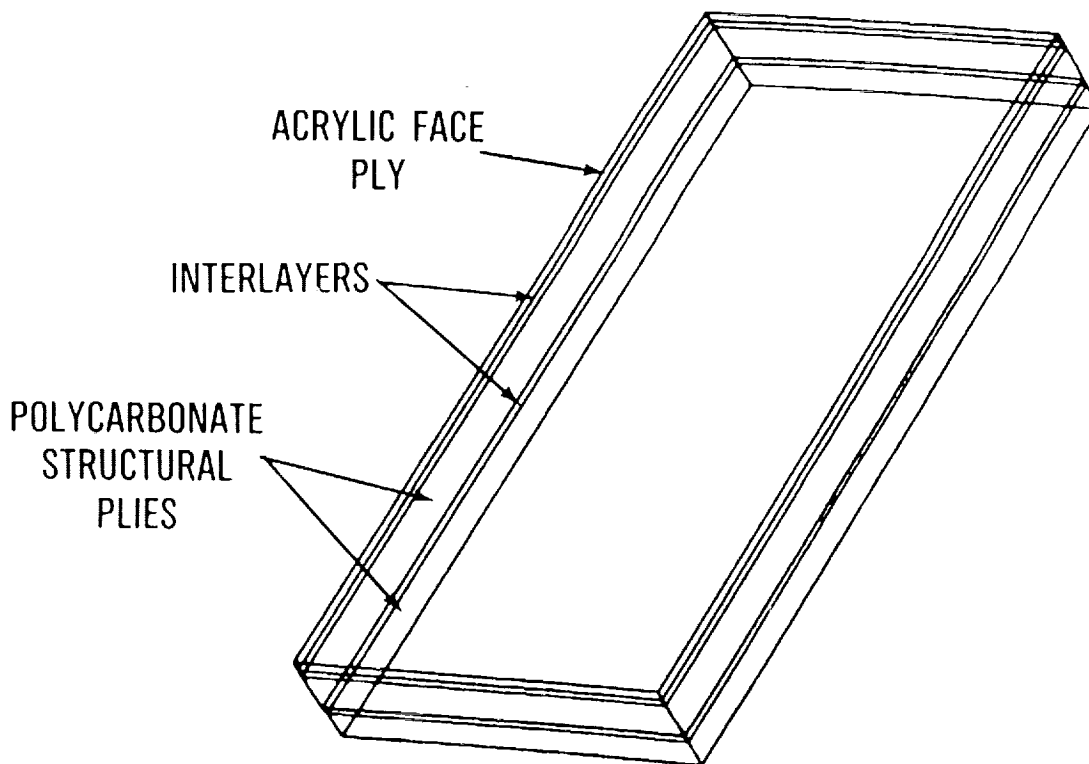
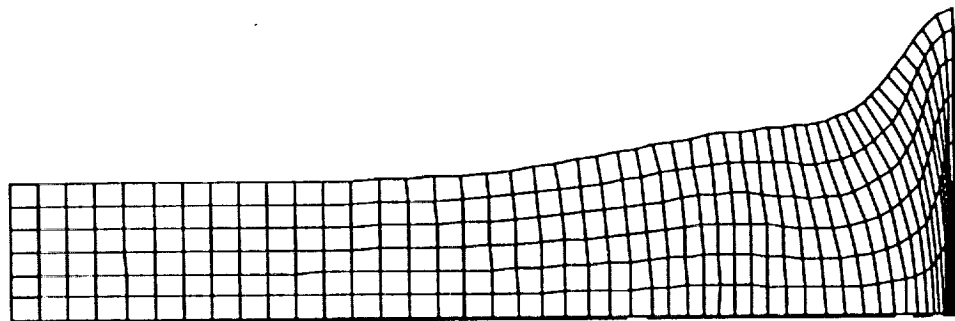


Figure 9 - Laminated windshield design for the T-46A aircraft.

TAYLOR CYLINDER SAMPLE ANALYSIS

The Taylor cylinder experiment, which is used to estimate the mechanical properties of metals at high strain rates, involves the normal impact of a cylinder onto a rigid surface. It is a common benchmark problem with a well-known solution. An X3D model was prepared for one quarter of the cylinder using 1350 8-node solid elements. Material constants typical of copper were used. Purely isotropic strain hardening was assumed, and no ultimate stress was specified (i.e., elements could not fail during the solution). Virtually all of the kinetic energy of the cylinder is dissipated through plastic deformation within about 80 microseconds. Figure 10 shows a deformed mesh plot of the cylinder in its final state.



TAYLOR CYLINDER - R = 3.2 MM, L = 32.4 MM - DOUBLE SYMMETRY
DISPLACEMENTS FOR TIME STEP = 8886 / TIME = 8.0000000E-05
11/13/90 22:53:12

Figure 10 - Deformed geometry of Taylor Cylinder.

TAYLOR CYLINDER SAMPLE ANALYSIS

Figure 11 shows a time history of the cylinder's length. The analysis was performed in 8886 time steps, and required 6 hours, 36 minutes on a VAX 8650 computer (about 0.00198 CPU seconds per element time step). The same analysis runs in about 40 minutes on a CRAY X-MP (.0002 seconds per element time step). Results from the X3D solution compare very well with analyses using the DYNA and NIKE codes, as shown below.

QUANTITY	X3D	DYNA2D	DYNA3D	NIKE2D
Final length, mm	21.47	21.47	21.47	21.47
Maximum radius, mm	7.081	7.127	7.034	7.068
Maximum strain at center	2.95	3.05	2.95	2.97

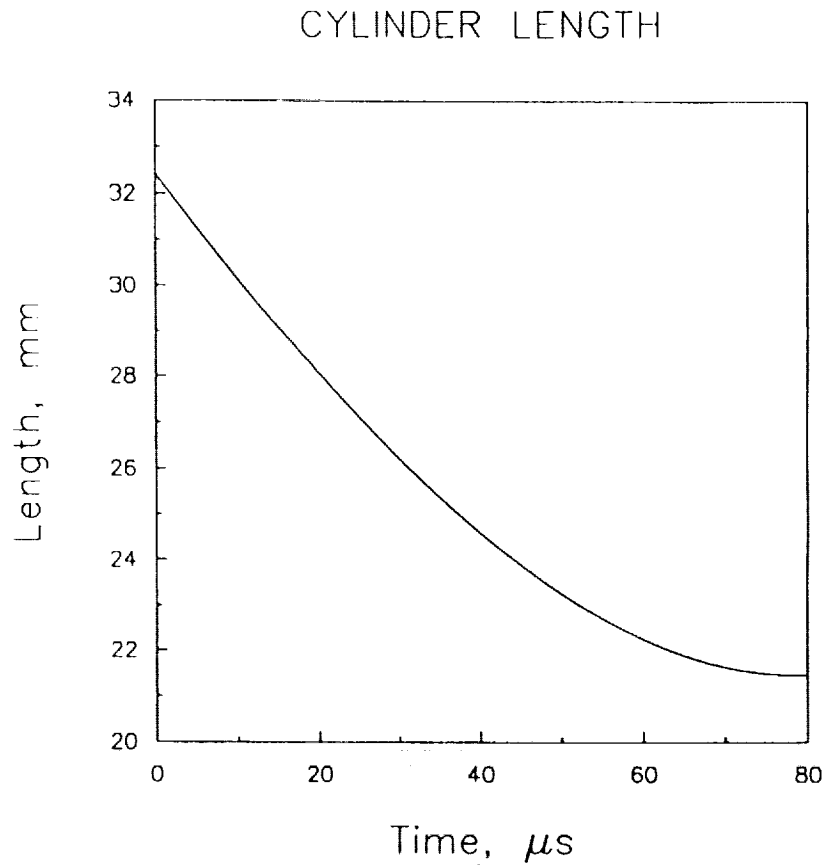


Figure 11 - Cylinder length versus time.

EXPLOSIVELY LOADED CYLINDRICAL SHELL SAMPLE ANALYSIS

Marchertas and Belytschko present both computational and experimental results for this problem (Ref. 10). A 120 degree cylindrical panel is loaded by igniting a charge spread over most of the surface. In the numerical solution, we represent this impulsive loading by a uniform initial velocity along the radius of the shell. A three point integration through the thickness of the shell was used with X3D. This is the minimum thickness integration order, and may give a solution which is slightly too flexible. Figure 12 shows the geometry of the explosively loaded cylindrical shell. The geometric and material parameters for the shell were:

Radius	2.9375 in.	Tensile modulus	10,500,000 psi
Thickness	0.125 in.	Density	0.0965 lb/cu.in.
Length	12.56 in.	Yield stress	44,000 psi
Velocity	5,650 in./sec (initial)		

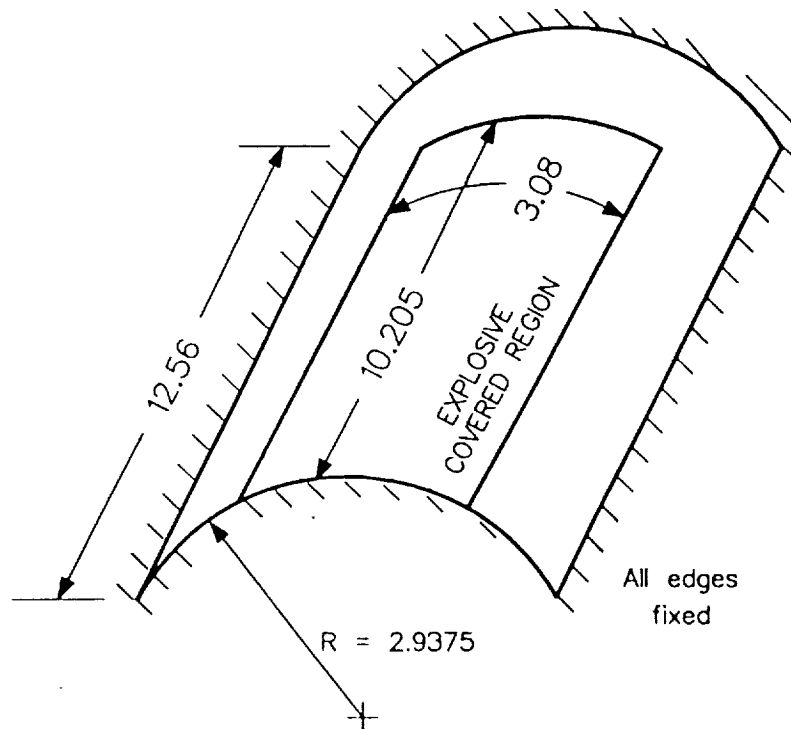


Figure 12 - Geometry of explosively loaded cylindrical shell.

EXPLOSIVELY LOADED CYLINDRICAL SHELL SAMPLE ANALYSIS

Results of the X3D solution, which was performed in 886 time steps, are shown in Fig. 13. The response mainly involves a flattening of the inner portion of the shell, consisting mostly of permanent deformation. The displacements peak at around 0.4 ms, with the largest inward displacements approaching half the radius. After this point, there is some elastic recovery (lasting about another 0.1-0.2 ms), but only very small vibration, since most of the energy has been dissipated through plastic flow. Displacement histories at selected points agree quite well with experimental results. Note that the initial velocity components are directed radially inward, and that points on the edges of the loaded region were assigned half the nominal initial velocity to provide the correct impulse to the shell.

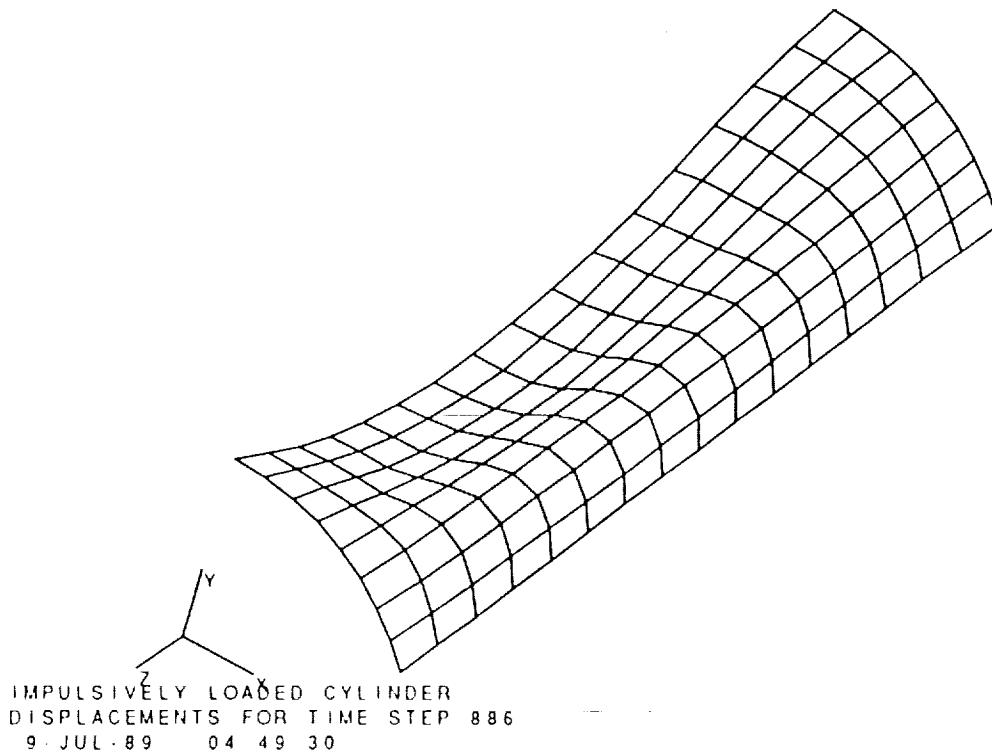


Figure 13 - Final deformed shape of cylindrical shell.

F-16 AIRCRAFT CANOPY BIRD IMPACT SAMPLE ANALYSIS

The F-16 bubble canopy provides a useful example for validation since the impact response involves very large motions, and the coupling between the load distribution and the deformation is strong. As a first step in validating the X3D code for bird impact simulation, several analyses of centerline impacts were carried out for the original production canopy, a 0.5 in. thick monolithic polycarbonate design. This design is capable of defeating 4 lb bird impact at airspeeds up to about 350 knots. Figure 14 shows the geometry of the transparency and of the projectile, a 4 lb bird idealized as a right circular cylinder. The patch outlined around the crown of the canopy and the entire bird are covered with contact elements. The canopy model consists of 928 quadrilateral plate elements. The bird is represented by 960 tetrahedral solids with equation-of-state coefficients typical of water, and very small shear stiffness and strength. The *low-strength* bird model, used in about half of the simulations, produces a pressure-volume response similar to water, and a "brittle" shear behavior. The ultimate and yield stresses coincide, so that element failure occurs at relatively small strains.

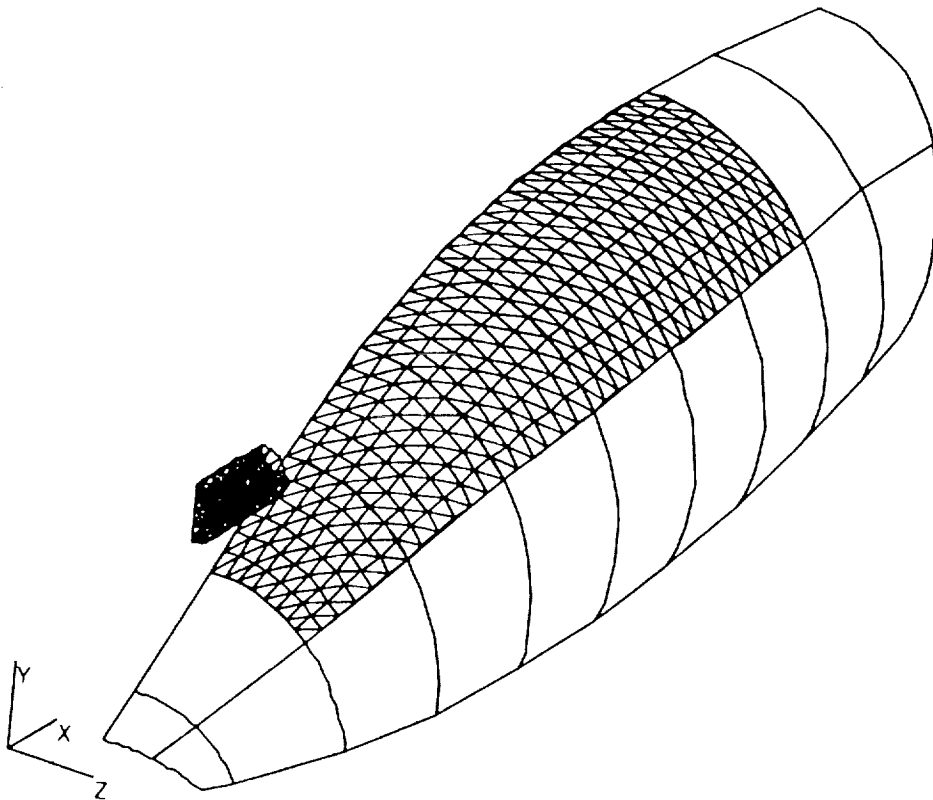


Figure 14 - Contact element grid for bird impact problem.

F-16 AIRCRAFT CANOPY BIRD IMPACT SAMPLE ANALYSIS

A *high-strength* bird model was used as well, which permits roughly 500% plastic (deviatoric) strain before the material is declared failed. The question of which bird model is more realistic has not been resolved because so many details are unknown with regard to material properties, precise support conditions, and center of impact location. Note that when elements of the bird model fail due to large shear distortion, their mass is retained in the problem, and the corresponding nodes continue to be used in contact calculations. Therefore, portions of the impacting body which have "failed" continue to transfer momentum to the target, but do not contribute to the summation of internal forces. In the deformed plot shown in Fig. 15, nodes attached to failed elements in the bird model are shown as small circles representing the center of mass positions. For the cases considered, the center of impact is at fuselage station 112 (measured in inches), which is about two feet aft of the forward edge of the canopy. The initial velocity of the bird is horizontal and equal to 350 knots (7,094 in./sec) at all nodes. The solution illustrated in Fig. 15 employs the low-strength bird. The displacement results are similar to experimentally observed values, although the computed deformed shape exhibits larger displacements in the forward region.

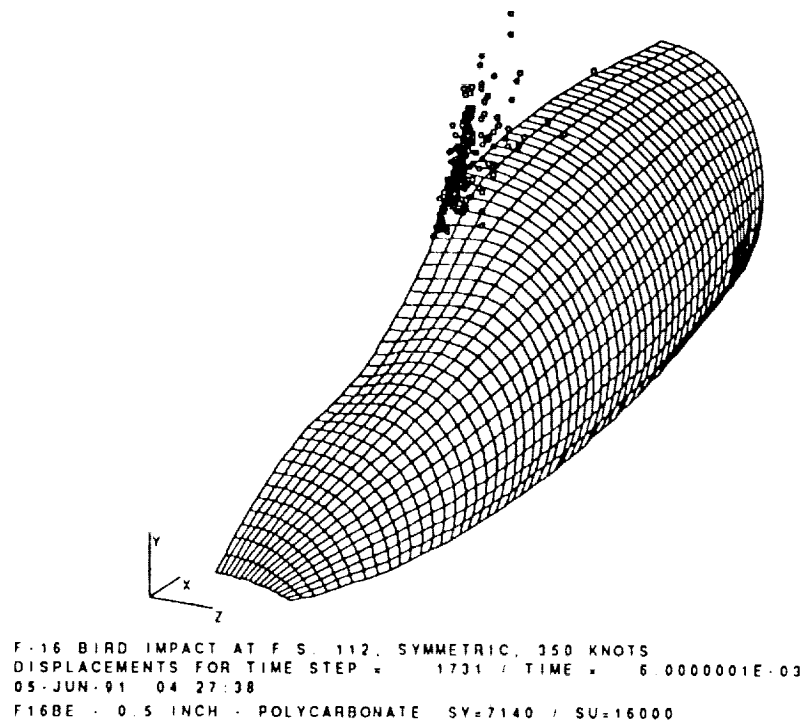


Figure 15 - Deformed geometry of F-16 canopy for low-strength bird 350 knot impact.

SUMMARY AND CONCLUSIONS

An improved analytical capability for soft-body impact simulation has been developed. Advances have been made in modeling impact loads, nonlinear materials, and layered wall constructions. The explicit approach adopted exploits the strengths of the current generation of supercomputer hardware, so that analysis cost and turnaround times are reduced significantly over the previous generation of bird impact analysis software. Experience in performing applications indicates that the solution methodology is very reliable, requiring minimal user intervention to avoid or correct problems with the solution. Implicit methods used in earlier work on these problems demand a great deal of user attention for stable, accurate, and convergent results, while the explicit technique is relatively trouble-free. The work reported here is a significant step toward a reliable capability for design screening and parametric investigation. Figure 16 lists the two primary research needs required to complete such a capability. With a modest effort in these areas of research need, the techniques and software described can become a truly useful and reliable tool for design and evaluation of a new generation of bird-impact resistant aircraft transparency systems.

- *Model Validation.* Additional comparisons of analytical predictions with full-scale impact test data are needed to develop confidence in the accuracy of the analysis and knowledge of its limitations.
- *Materials Characterization.* The transparency materials in wide use are high-polymer compounds with very complex characteristics. Much more experimental and analytical work is needed to understand these materials adequately and model their behavior faithfully.

Figure 16 - Research needs for aircraft transparency bird impact, explicit finite element analysis methods.

REFERENCES

1. Brockman, R. A., *MAGNA (Materially And Geometrically Nonlinear Analysis), Part I - Finite Element Analysis Manual*. AFWAL-TR-82-3098, Part I, 1982.
2. McCarty, R. E., *MAGNA Computer Simulation of Bird Impact on the TF-15 Aircraft Canopy*. AFWAL-TR-83-4154, 1983.
3. McCarty, R. E., *Analytic Assessment of Bird Impact Resistant T-46A Aircraft Windshield System Designs using MAGNA*. WRDC-TR-89-4044, 1989.
4. McCarty, R. E., *MAGNA Analysis of Space Shuttle Orbiter Windshield System Bird Impact Protection*. WRDC-TR-89-4044, 1989.
5. Bouchard, M. P., *Finite Element Analysis of the B-1B Windshield System*. WRDC-TR-89-4044, 1989.
6. Flanagan, D. P. and Belytschko, T., "A Uniform Strain Hexahedron and Quadrilateral with Orthogonal Hourglass Control," *International Journal for Numerical Methods in Engineering*, Vol. 17, 1981, pp. 679-706.
7. Brockman, R. A., *Finite Element Analysis of Soft-Body Impact*. AFWAL-TR-84-3035, 1984.
8. Belytschko, T., Lin, J. I. and Tsay, C. S., "Explicit Algorithms for the Nonlinear Dynamics of Shells," *Computational Methods in Applied Mechanics and Engineering*, Vol. 42, 1984, pp. 225-251.
9. Hughes, T. J. R., Cohen, M. and Haroun, M., "Reduced and Selective Integration Techniques in the Finite Element Analysis of Shells," *Nuclear Engineering Des.*, Vol. 46, 1978, pp. 203-222.
10. Marchertas, A. H. and Belytschko, T., *Nonlinear Finite Element Formulation for Transient Analysis of Three-Dimensional Thin Structures*. ANL-8104, 1974.

